

AN EVALUATION OF MULTIAXIAL FATIGUE DATA FROM TI-6AL-4V USING A CRITICAL PLANE METHODOLOGY

M. Erickson¹, A. Kallmeyer¹, E. Goodin¹, E. Torkelson¹, and P. Kurath²

¹Department of Mechanical Engineering, North Dakota State University,
Fargo, ND 58105, USA

²Department of Mechanical Engineering, University of Illinois,
Urbana, IL 61801, USA

ABSTRACT

The prediction of fatigue life or allowable stress levels for metallic components under complex, multiaxial stress states is a challenging aspect in design. While equivalent-stress approaches often work reasonably well for simple proportional load paths, the analysis of non-proportional load paths brings forth additional complexities, such as the identification of cycles and the definition of mean stresses. Critical plane approaches, in which the orientation of the plane on which the crack will nucleate is taken into consideration, have shown better success in correlating experimental results under a wide variety of load paths. However, while the interpretation of the stress terms in a critical plane parameter is generally straightforward within proportional loadings, there is often ambiguity in the definition when the loading is non-proportional. In this paper, a thorough examination of the variables responsible for crack nucleation is presented in the context of the critical plane methodology. Uniaxial and multiaxial fatigue data from Ti-6Al-4V are used as the basis for the evaluation. The experimental fatigue data include axial, torsional, proportional tension/torsion, and a variety of non-proportional tension/torsion load paths. Specific attention is given to the effects of torsional mean stresses, critical plane definition, and the interpretation of normal stress terms on the critical plane within non-proportional load paths. A new critical plane parameter is presented that provides good correlation with the fatigue data.

KEYWORDS

Multiaxial fatigue, critical plane, non-proportional loading, titanium, mean stresses.

INTRODUCTION

Many critical engineering components, such as axles, crankshafts, turbine disks and blades, and notched components, are routinely subjected to cyclic multiaxial stress states. Given the complexity and expense of conducting multiaxial fatigue tests that simulate realistic loading conditions, the reliable design of such components requires that accurate models be available that can relate cyclic multiaxial loading conditions to uniaxial fatigue data. These methods must be capable of modeling the accumulation of fatigue damage under a variety of conditions, including non-proportional loading (i.e., when the principal stress directions rotate during a cycle of loading), and in the presence of multiaxial mean stresses.

A significant amount of research has been devoted over the past few decades towards gaining a better understanding of the mechanisms by which fatigue damage accumulates under multiaxial loading, and to the development of damage parameters to model the observed behavior [1,2]. The majority of these models can be broadly classified into equivalent-stress based models, energy-based damage theories, or critical plane parameters. Most equivalent stress models are derived from extensions of static yield theories. The advantage of these models lies in their relative simplicity of implementation, as a scalar parameter is used to represent all components in the cyclic stress tensor. The energy-based theories, in general, also utilize a scalar parameter (e.g., distortion energy or plastic work per cycle) as a measure of fatigue damage. A shortcoming of both classes of models is in their inability to portray the physics of the damage process. Empirical evidence has shown that cracks nucleate and grow along preferred orientations, or planes, in the material. However, a scalar parameter cannot distinguish between planes on which cracks may form.

Critical plane models have been developed in an attempt to interpret the physical mechanisms governing the nucleation and growth of small fatigue cracks [3]. In using these parameters, damage is calculated in terms of cyclic stresses or strains on each plane within the material to identify the plane containing the greatest amount of damage, or alternatively on planes experiencing the maximum level of a predetermined value, such as cyclic shear stress. In a previous study conducted by the authors [4], critical plane models were found to provide generally better agreement with multiaxial fatigue data for Ti-6Al-4V generated as part of a U.S. Air Force initiative dedicated to the improvement of HCF life prediction methodologies.

In the present study, a detailed analysis of biaxial (tension/torsion) fatigue data for Ti-6Al-4V is presented within the framework of the critical-plane methodology. Specific attention is given to complicating factors such as mean stress effects (including torsional mean stresses), non-proportional load paths, and the presence of secondary stress fluctuations within the dominant cycle on the critical plane. A new critical-plane damage parameter is proposed that is based on a physical interpretation of the damage process, and which shows an improved correlation of the biaxial and uniaxial fatigue data for Ti-6Al-4V.

BACKGROUND

Material and Test Program

The critical plane analysis was formulated using the results of an extensive set of uniaxial and biaxial fatigue data for Ti-6Al-4V that was generated as part of the U.S. Air Force National HCF Science and Technology Program. This data set consisted of uniaxial fatigue data at stress ratios of $R = -1, 0.1,$ and $0.5,$ and approximately 30 biaxial (tension/torsion) tests that encompassed a variety of mean stress conditions and non-proportional load paths. The biaxial tests were conducted in strain control using smooth, solid specimens with a gage section diameter of 12.5 mm. For these tests, the stresses used in the analysis represent stabilized, half-life values on the outer surface of the specimen. Most specimens experienced only elastic strains during the cyclic loading. For these specimens, the surface stresses were obtained analytically from measured load and torque values. However, a few specimens did incur plastic strains on the first reversal. An elastic-plastic finite element analysis was performed for those tests, which made use of a multilinear kinematic hardening rule with a Ramberg-Osgood representation of the cyclic stress-strain curve. The material properties used in the analysis are shown in Table 1. More details on the material and experimental procedures can be found in Ref [4].

TABLE 1
MATERIAL PROPERTIES FOR TI-6AL-4V

| Property | Value |
|---|---------|
| Modulus of elasticity (E) | 116 GPa |
| Cyclic strain hardening coefficient (K') | 854 MPa |
| Cyclic strain hardening exponent (n') | 0.0149 |
| 0.2% offset cyclic yield strength (σ_y') | 750 MPa |
| 0.2% offset monotonic yield strength (σ_y) | 930 MPa |
| Ultimate strength (σ_{ut}) | 977 MPa |

The biaxial data included torsion tests at $R = -1, 0.1, \text{ and } 0.5$, proportional load paths, and a variety of non-proportional load paths as shown in Figure 1. These figures illustrate the applied loading in tension/torsion (σ/τ) space throughout one cycle. In the case of the check path, the sample is loaded to the top of the curve, and then unloaded along the same path. Both the level of loading and shape of the non-proportional paths were intended to simplify portions of actual service events encountered in turbine engine components.

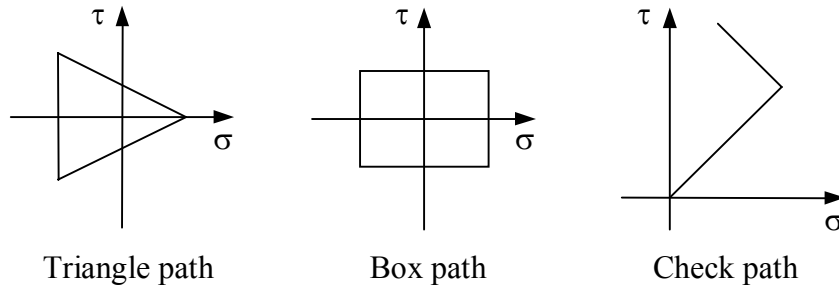


Figure 1: Non-proportional biaxial load paths.

Findley Critical Plane Parameter

In a previous study [4], the authors evaluated over 20 multiaxial fatigue damage models by comparison of the biaxial Ti-6Al-4V data with a baseline curve obtained by fitting the uniaxial test data at different stress ratios. From this analysis, a critical plane model proposed by Findley [5] was shown to provide reasonably good correlation of the biaxial and uniaxial fatigue data. The Findley parameter characterizes damage on a given plane by addition of the maximum shear stress amplitude (τ_a) and the maximum normal stress (σ_{\max}), multiplied by an adjustable factor (k) on that plane. The plane on which crack nucleation is assumed to begin, or critical plane, is then defined as the plane that experiences the maximum value of this parameter. The Findley Parameter (FP) is defined as shown in Eqn. 1, where a dual power-law relation was used to fit the experimental data:

$$FP = \tau_a + k\sigma_{\max} = AN^b + CN^d \quad (1)$$

In Eqn. 1, N represents the cycles to failure and $A, b, C,$ and d are curve fitting constants. Application of the Findley model to the uniaxial and biaxial data sets is shown in Figure 2. The curve shown in these figures represents a best fit to the uniaxial data set only, obtained from Eqn. 1. Note that the majority of the biaxial data collapse reasonably well about the uniaxial curve. However, the data for the box path fall above the curve, indicating the Findley parameter produces an overly conservative life prediction for this load path.

CRITICAL PLANE ANALYSIS

In the development of his parameter, Findley [5] postulated that the nucleation and growth of small fatigue cracks were driven primarily by cyclic shear stresses, which has been verified by experimental observations of slip band formation under shear loading within individual grains. The normal stress on the plane of cyclic shear stress was considered to have a secondary effect by separating the crack surfaces if tensile, thereby reducing crack face interaction during shear crack growth. However, the Findley parameter fails to fully capture certain characteristics of the loading that can occur under complex, non-proportional load paths. These effects can be observed through careful examination of experimental data, including torsional mean stresses, the phase characteristics between the shear and normal stresses, and the influence of cyclic normal stresses on the critical plane. In the following sections, these effects are discussed and accounted for in the development of a new critical plane parameter.

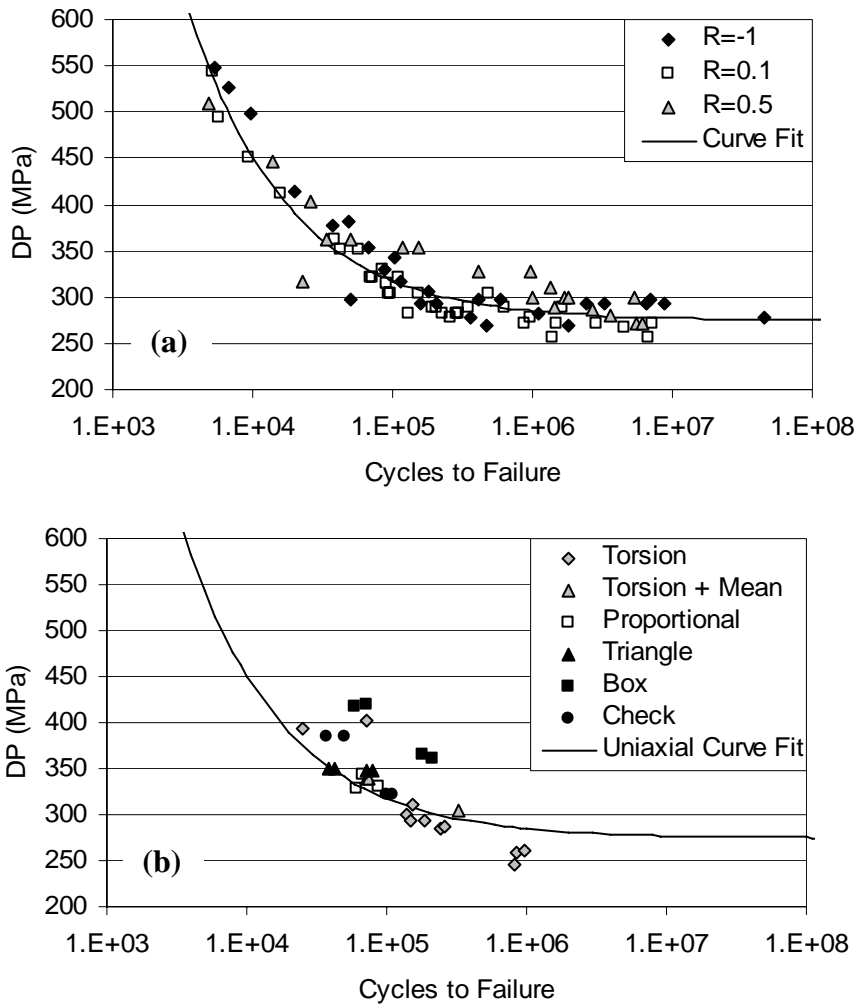


Figure 2: Findley parameter applied to (a) uniaxial and (b) biaxial Ti-6Al-4V fatigue data.

Torsional Mean Stresses

It is commonly assumed that torsional mean stresses have no effect on the torsional fatigue strength of metals, based on experimental studies involving load levels near the endurance limit of steel alloys [6]. However, it has been reported that when the maximum shear stress approaches roughly 80% of the torsional yield strength, the presence of a mean shear stress may have a deleterious effect on the allowable shear stress amplitude [7].

To examine the effect of torsional (shear) mean stresses in Ti-6Al-4V, the torsion data at $R = -1, 0.1,$ and 0.5 were evaluated. The shear stress amplitude is plotted vs. cycles to failure for this set of data in Figure 3(a). As is evident from this figure, there is clearly a mean shear stress effect on the allowable shear amplitude between $R = -1$ and 0.1 , although the effect is less pronounced between $R = 0.1$ and 0.5 . To account for the influence of mean shear stresses, an effective shear stress amplitude is defined as

$$\tau_{eff} = |\tau_{max}| \left(1 - \frac{\tau_{min}}{\tau_{max}} \right)^w \quad (2)$$

where w is a material parameter that can be adjusted to account for the influence of mean shear stress. This parameter can range in value from 0 (high mean stress effect) to 1 (no mean stress effect). Applying Eqn. 2 to collapse the torsional data in Figure 3(a) results in a value of $w = 0.66$ for Ti-6Al-4V. The effective shear stress amplitude is plotted in Figure 3(b). As can be seen, Eqn. 2 provides a good representation of the torsional fatigue data, accounting for mean shear stress effects.

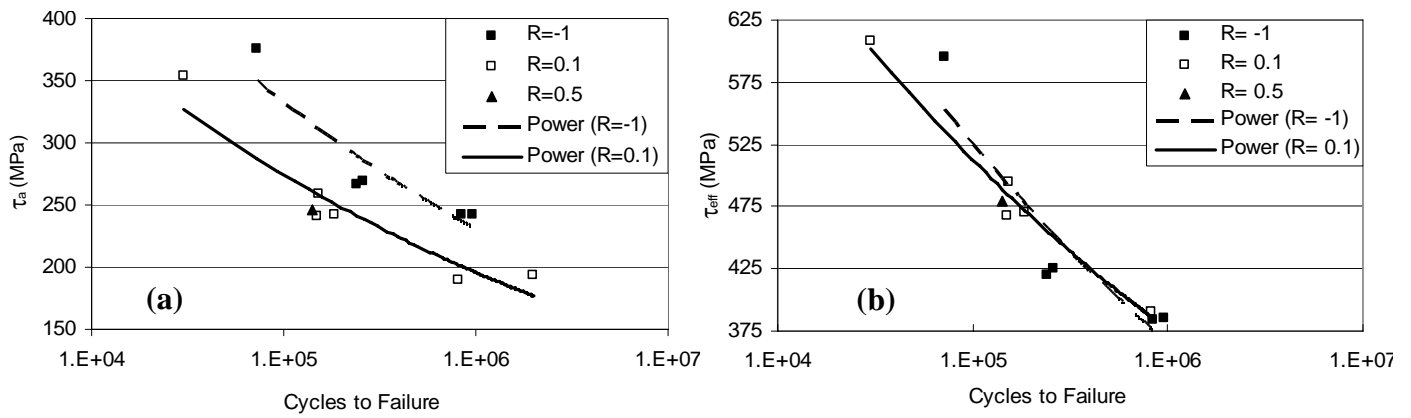


Figure 3: Effect of mean shear stress on torsional fatigue strength: (a) shear stress amplitude and (b) effective shear stress amplitude vs. cycles to failure.

Effect of Normal Stress on Maximum Shear Plane

Figure 4 illustrates the role of normal stresses on the critical plane of selected specimens, and in particular the interaction of the normal and shear stresses. All of the stresses in this figure are taken from the plane of maximum shear stress amplitude for ease of comparison, and specimens with similar shear amplitudes were selected so that the only significant difference between the cycles is the normal stress contribution. The ‘reversed torsion’ cycle (solid diamond) serves as a good baseline because it has no normal stress influence, and it has a life of 250,000 cycles. The ‘torsion mean tension’ cycle (solid square) also consists of reversed torsion, but a constant tensile normal stress of 100 MPa is superimposed on the torsion cycle. This normal stress is detrimental even though it is not cyclic, causing a reduction in life by a factor of 3.4, to 73,000 cycles. Since the constant tensile normal load alone would not cause a fatigue failure, it is believed that the role of this load is to open the nucleating cracks in the material. This opening reduces the level of crack face interaction, thereby lowering the amount of resistance that must be overcome by the cyclic shear stress in order to cause damage. The shear stress therefore has the ability to cause more damage, possibly because it begins causing the damage at an earlier (lower stress) point in the cycle, it causes a higher level of damage at the peak shear stress levels, or most likely some combination of the two.

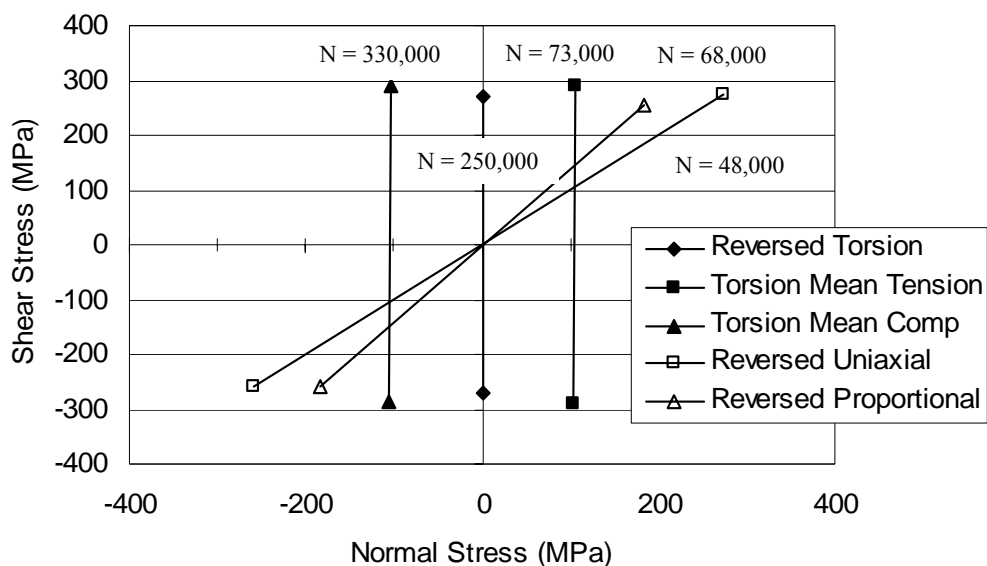


Figure 4: Load paths on plane of maximum shear stress amplitude for specimens with similar shear amplitudes.

The ‘torsion mean compression’ load path (solid triangle) shown in Figure 4 is similar to the previous load path, except the normal stress is compressive rather than tensile. As expected, this compressive normal stress is beneficial, increasing the life of the specimen by a factor of 1.3 to 330,000 cycles. Similarly, the suspected reason for the beneficial effect is due to the nucleating cracks being closed by the normal stress,

which would increase crack face interaction and the resistance that opposes the cyclic shear stress. It is important to note, however, that the increase in life resulting from the application of a compressive normal stress is not equal to the reduction in life observed from the application of a tensile normal stress of equal magnitude.

The two aforementioned specimens indicate the need for a damage parameter that takes into account both the detrimental and beneficial effects of a constant normal stress superimposed on a cyclic shear stress. This was done by multiplying the τ_{eff} term in Eqn. 2 by an adjustment factor as follows:

$$DP = |\tau_{max}| \left(1 - \frac{\tau_{min}}{\tau_{max}} \right)^w \left(1 + \frac{k_o \sigma_1 + k_o \sigma_2}{\sigma_y} \right) \quad (3)$$

In this equation, σ_1 and σ_2 are the normal stresses at the shear reversal points (which are the max and min points for both normal and shear stresses in proportional loading, as shown in Figure 4), σ_y is the yield strength of the material, and k_o is a curve fitting parameter. In the case where the normal stress is zero at the shear reversal points, this multiplier term is simply one. Therefore it drops out of the equation as it should for that scenario. As mentioned above, Figure 4 indicates that a tensile normal stress is detrimental, and a compressive normal stress is beneficial. However, the differences are not equal. The tensile normal stress reduced the life by a factor of 3.4, whereas the compressive normal stress with an identical magnitude increased the life by only a factor of 1.3. Hence there is a need for the damage parameter to account for this imbalance. This is achieved by defining k_o as follows:

$$k_o = \begin{cases} k^+ & \text{if } \sigma > 0 \\ k^- & \text{if } \sigma < 0 \end{cases} \quad (4)$$

Here the value of k_o is dependant upon the sign of the normal stress. If the normal stress is tensile, then k^+ is used, and if the normal stress is compressive, then k^- is used as the curve fitting parameter. This definition allows for the influence of a tensile normal stress to be larger than the influence of a compressive normal stress by allowing k^+ to be larger than k^- , with each of them being greater than zero. In addition, by separately accounting for the effect of the normal stress at each reversal point, rather than using just the maximum normal stress throughout the cycle as in Eqn. 1, the influence of a varying normal stress can be better modeled.

Now considering the ‘reversed uniaxial’ (hollow square) and the ‘reversed proportional’ (hollow triangle) load paths in Figure 4, we can see that their normal stresses are cyclic on the max shear plane. The uniaxial specimen has a higher max normal stress than the proportional specimen, and the lives reflect this trend with values of 48,000 and 68,000 cycles respectively. Interestingly, the proportional specimen has a similar life as the ‘torsion mean tension’ sample. The max normal stress is significantly higher for the proportional specimen, but the minimum normal stress is compressive. Therefore there is a combination of detrimental and beneficial effects occurring. Including a mean stress term cannot properly account for this effect because the mean normal stress for the proportional specimen is zero, whereas it is the constant 100 MPa for the ‘torsion mean tension’ specimen. The difference between the two samples that must be taken into consideration is the cycling normal stress. This influence is accounted for in the damage parameter of Eqn. 3 by adding another term similar in form to Eqn. 2, as shown below:

$$DP = |\tau_{max}| \left(1 - \frac{\tau_{min}}{\tau_{max}} \right)^{w_1} \left(1 + \frac{k_o \sigma_1 + k_o \sigma_2}{\sigma_y} \right) + k \sigma_{max}^+ \left(1 - \frac{\sigma_{min}^+}{\sigma_{max}^+} \right)^{w_2} \quad (5)$$

Since compressive cyclic normal stresses are commonly regarded as having a negligible contribution to the fatigue damage in comparison to the tensile cyclic normal stresses, only the tensile portions of the cyclic stresses are used in the second term shown above. In this term, σ_{max}^+ is the greater value between zero and the maximum normal stress in the cycle, σ_{min}^+ is the greater value between zero and the minimum normal

stress in the cycle, and k and w_2 are both curve fitting parameters, with w_2 assumed to be 0.5 in this study. The purpose of this term is to take into account the contribution of a cyclic normal stress on the maximum damage plane. One benefit to this configuration is that if there is no cyclic normal stress (as in the three aforementioned load paths), then σ_{\min}^+ is equal to σ_{\max}^+ and the entire second term becomes zero.

Under proportional loading, the max and min normal stresses occur at the same time as the max and min shear stresses (reversals), therefore the normal stresses used in the multiplier term and the additive term in Eqn. 5 are the same (unless there is a compressive normal stress, which would then be replaced by a zero in the second term). However, in nonproportional loading, the normal stresses may not be the same for each term. Figure 5 illustrates this type of scenario by showing the normal and shear stress histories on the maximum shear plane over one cycle of the check path. As indicated on the figure, the min shear stress (τ_A) does occur at the same time as the min normal stress (σ_A), however the max shear stress ($|\tau_B|$) does not occur at the same time as the max normal stress (σ_C). The stresses that are used in the multiplier term of the damage parameter are the normal stresses at shear reversal points (τ_A , τ_B) because these are the normal stresses that are helping or hindering the shear stress by holding the crack open or closed. Therefore, the normal stresses for the multiplier term would be σ_A and σ_B . However, for the additive term of the damage parameter, the max and min normal stresses over the cycle are used. In this case they would be σ_C and σ_A since both are greater than or equal to zero. If either or both of them were less than zero, they would be replaced by a zero in the damage parameter because the additive term only uses the positive values as described above.

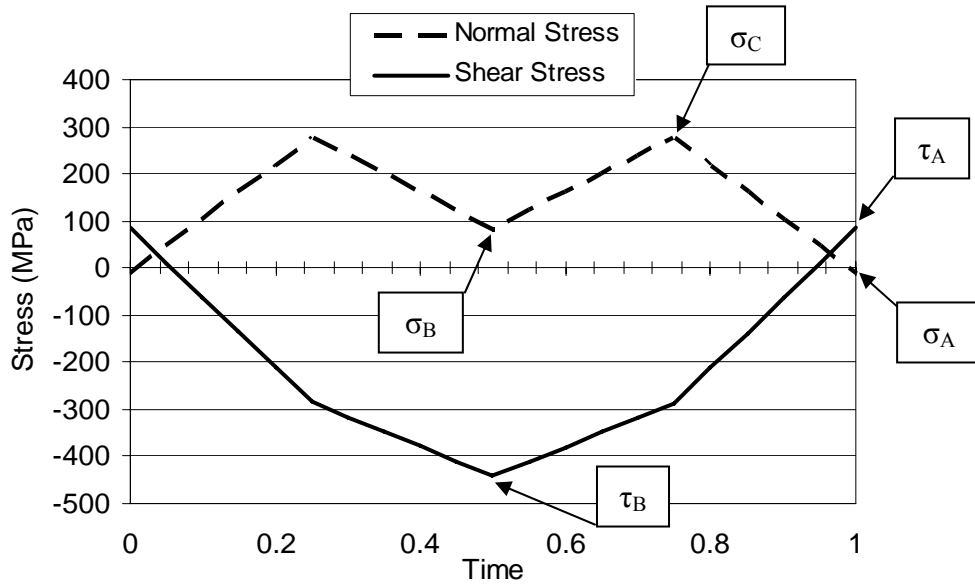


Figure 5: Normal and shear stresses vs. time for one shear cycle on the max shear amplitude plane of a check path specimen.

Examination of Figure 5 also brings forth another issue that must be addressed: multiple normal stress cycles within a shear stress cycle. For the check path, there are two normal stress cycles for every shear stress cycle as shown. In this case, each normal stress cycle shares the same maximum point, but they differ at the minimum point (using the Rainflow cycle counting procedure). To account for this effect, the damage parameter is amended to include a summation of the normal stress cycles. Therefore, the final form of the damage parameter is as follows:

$$DP = |\tau_{\max}| \left(1 - \frac{\tau_{\min}}{\tau_{\max}} \right)^{w_1} \left(1 + \frac{k_o \sigma_1 + k_o \sigma_2}{\sigma_y} \right) + k \sum \sigma_{\max}^+ \left(1 - \frac{\sigma_{\min}^+}{\sigma_{\max}^+} \right)^{w_2} \quad (6)$$

Application of the above damage parameter to the aforementioned Ti-6Al-4V uniaxial and biaxial data sets is shown in Figure 6. In this analysis, the damage parameter values were calculated on the maximum shear plane, rather than the maximum damage plane, to simplify the optimization routines used to determine the material parameters required in Eqn. 6. By applying an error-minimization analysis to the combined set of

uniaxial and biaxial data, these parameters were evaluated as $w_I = 0.68$, $k^+ = 0.75$, $k^- = 0.07$, and $k = 0.16$. The curve fit shown in Figure 6 represents a dual power law fit (as in Eqn. 1) to both the uniaxial and biaxial data. Overall, the uniaxial data are well centered on the prediction curve. There is some slight separation of stress ratios at longer lives; however the overall fit is an improvement over the Findley model shown in Figure 2. The damage parameter provides a good representation of the multiaxial data as well, with nearly all of the multiaxial data being within the scatter of the uniaxial data. With the exception of one point, the torsion data are well centered on the curve, and the torsion points with a mean tensile or compressive normal stress are very close to the curve. The proportional, triangle, and check path data points are slightly above the curve, but they are grouped well. Two of the four box paths are very near the curve, however the other two have an over-predicted amount of damage. Those two box paths are different from the load path shown in Figure 1 in that they are not centered about the origin. Instead they are shifted towards the left, or into a larger compressive normal stress and smaller tensile normal stress.

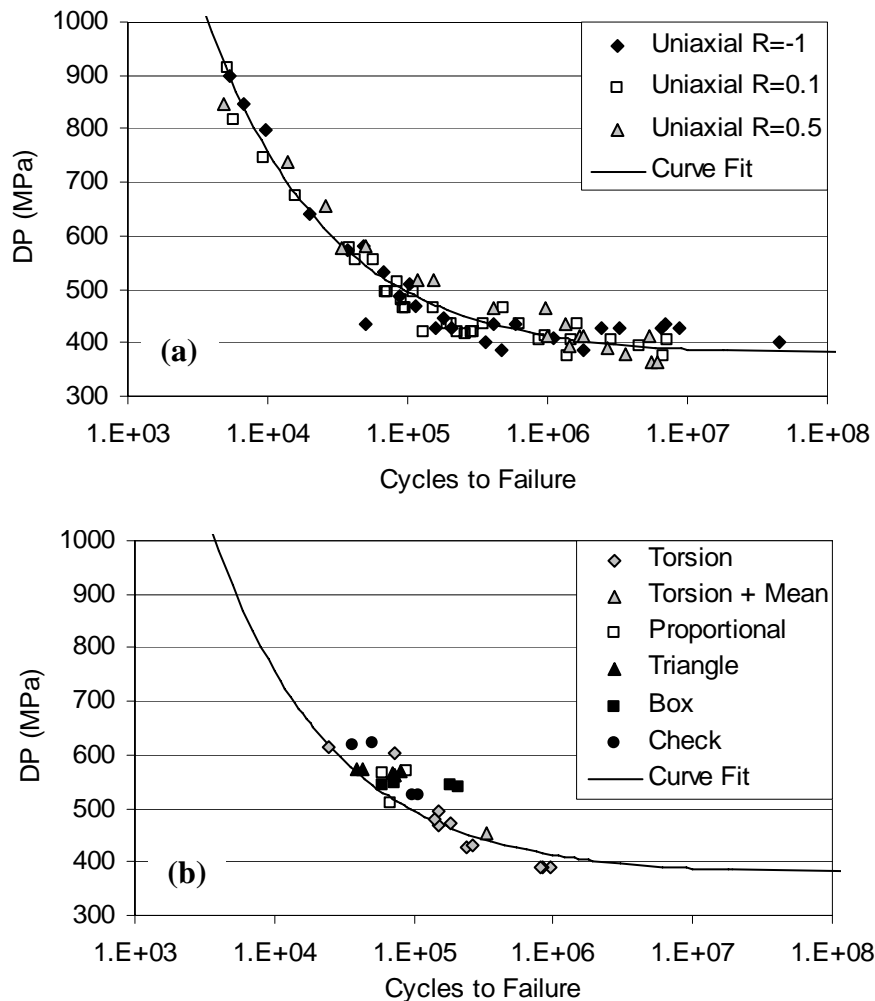


Figure 6: Proposed damage parameter applied to (a) uniaxial and (b) multiaxial Ti-6Al-4V fatigue data.

The proposed new multiaxial damage parameter given in Eqn. 6 and plotted in Figure 6 is based on a physical interpretation of the damage mechanisms observed under cyclic loading. Overall, this model provides a very good fit to the combined set of uniaxial and multiaxial fatigue data for Ti-6Al-4V. Furthermore, the application of this parameter on the maximum shear plane rather than the maximum damage plane simplifies the implementation of this parameter within a design code, as it generally requires less computational effort to identify the plane of maximum cyclic shear stress.

CONCLUSION

A thorough examination of biaxial (tension/torsion) fatigue data for Ti-6Al-4V has been undertaken to identify the parameters that contribute to the accumulation of fatigue damage under multiaxial loading. It is

evident from this analysis that, within the stress ranges tested, a torsional (shear) mean stress effect exists in this material. Through comparison of several key tests, the influence of the static and cyclic components of the normal stress on shear crack nucleation has been explained. A new multiaxial critical plane parameter has been proposed that is based on a physical interpretation of fatigue damage mechanisms. This parameter, when calculated on the plane of maximum shear stress amplitude, provides a very good correlation to a large set of uniaxial and biaxial Ti-6Al-4V fatigue data, including several non-proportional load paths.

REFERENCES

1. Garud, Y.S. (1981) *J. Test. and Eval.* 9, 165.
2. You, B.R. and Lee, S.B. (1996) *Int. J. Fatigue*, 18, 235.
3. Socie, D. (1993). In: *Advances in Multiaxial Fatigue, ASTM STP 1191*, pp. 7-36, McDowell, D.L. and Ellis, R. (Eds.). American Society for Testing and Materials, Philadelphia.
4. Kallmeyer, A.R., Krgo, A., and Kurath, P. (2002) *J. Eng. Mat. and Tech.*, 124, 229.
5. Findley, W.N. (1957) *ASME Transactions*, 79, 1337.
6. Davoli, P., Bernasconi, A., Filippini, M., Foletti, S., and Papadopoulos, I.V. (2003) *Int. J. Fatigue*, 25, 471.
7. Sines, G. and Ohgi, G. (1981) *J. Eng. Mat. and Tech.*, 103, 82.